

VU Research Portal

Molecular mechanisms of toxic effects of fotemustine in rat hepatocytes and subcellular rat liver fractions.

Brakenhoff, J.P.G.; Commandeur, J.N.M.; Wormhoudt, L.W.; Groot, E.J.; Vermeulen, N.P.E.

published in

Carcinogenesis
1996

DOI (link to publisher)

[10.1093/carcin/17.4.715](https://doi.org/10.1093/carcin/17.4.715)

document version

Publisher's PDF, also known as Version of record

[Link to publication in VU Research Portal](#)

citation for published version (APA)

Brakenhoff, J. P. G., Commandeur, J. N. M., Wormhoudt, L. W., Groot, E. J., & Vermeulen, N. P. E. (1996). Molecular mechanisms of toxic effects of fotemustine in rat hepatocytes and subcellular rat liver fractions. *Carcinogenesis*, 17(4), 715-724. <https://doi.org/10.1093/carcin/17.4.715>

General rights

Copyright and moral rights for the publications made accessible in the public portal are retained by the authors and/or other copyright owners and it is a condition of accessing publications that users recognise and abide by the legal requirements associated with these rights.

- Users may download and print one copy of any publication from the public portal for the purpose of private study or research.
- You may not further distribute the material or use it for any profit-making activity or commercial gain
- You may freely distribute the URL identifying the publication in the public portal ?

Take down policy

If you believe that this document breaches copyright please contact us providing details, and we will remove access to the work immediately and investigate your claim.

E-mail address:

vuresearchportal.ub@vu.nl

Molecular mechanisms of toxic effects of fotemustine in rat hepatocytes and subcellular rat liver fractions

Jan P.G.Brakenhoff, Jan N.M.Commandeur,
Lars W.Wormhoudt, Ed J.Groot and
Nico P.E.Vermeulen¹

Leiden/Amsterdam Center for Drug Research, Division of Molecular
Toxicology, Free University, De Boelelaan 1083, 1081 HV Amsterdam,
The Netherlands

¹To whom correspondence should be addressed

Fotemustine is a clinically used DNA-alkylating 2-chloroethyl-substituted *N*-nitrosourea, which sometimes shows signs of haematotoxicity and reversible liver and renal toxicity as toxic side-effects. Mechanistic data on these side-effects are scarce and incomplete. In this study, firstly the cytotoxicity of fotemustine in freshly isolated rat hepatocytes was investigated and secondly the metabolism of fotemustine and possible mechanisms involved in the observed cytotoxicity. Fotemustine caused concentration- and time-dependent cytotoxic effects in rat hepatocytes. Extensive GSH-depletion and formation of GSSG were first observed, followed by lipid peroxidation and finally by cell death measured as LDH-leakage. 2-Chloroethyl analogues of fotemustine, which in contrast to fotemustine have no carbamoylating potency, were not toxic to rat hepatocytes. The data suggest that the cytotoxicity of fotemustine is resulting from its reactive decomposition product, DEP-isocyanate. GSH-conjugation of DEP-isocyanate was shown to protect against the cytotoxicity of fotemustine, however, only temporary and not completely. Synthetical DEP-SG, the GSH-conjugate of DEP-isocyanate, was also toxic to rat hepatocytes, albeit to a significantly lesser extent than fotemustine. In rat liver microsomes, no fotemustine-induced LPO was observed, suggesting that reactive decomposition products of fotemustine do not directly cause peroxidation of cellular membranes. Fotemustine did not affect the antioxidant enzymes superoxide dismutase, catalase, GSH-peroxidase, GSSG-reductase and GSH S-transferases. Thus, direct effects on

these antioxidant enzymes are not likely to explain the cytotoxic effects of fotemustine in hepatocytes. In conclusion, it is proposed that the cytotoxicity of fotemustine in rat hepatocytes is caused by rapid and extensive depletion of GSH by DEP-isocyanate, a reactive decomposition product of fotemustine, consequently hampering the endogenous protection against its own toxicity. Knowledge of molecular mechanisms of the cytotoxicity of fotemustine may contribute to a more rational design of selective protection against toxic side-effects which occur upon therapy of patients with fotemustine.

Introduction

Fotemustine is a DNA-alkylating 2-chloroethyl-substituted *N*-nitrosourea (CENU*) (Figure 1) (1). The chemotherapeutic drug is known to decompose rapidly into 2-chloroethyldiazohydroxide and diethyl (1-ethyl)phosphonate (DEP)-isocyanate (2). 2-Chloroethyldiazohydroxides can chloroethylate endogenous nucleophilic sites of macromolecules such as DNA (3). Reactive isocyanates of CENUs have been suggested to cause toxic effects (4,5) by carbamoylation of thiols and primary amines of proteins and enzymes, such as chymotrypsin (6), adenosine triphosphatase, acetylcholinesterase (7) and GSSG-reductase (8). Different isocyanate-related toxicities have meanwhile been reported. Genotoxic effects such as chromosome aberrations, sister chromatid exchanges, mutations and/or cancer are known (9). In rats and rabbits, methyl isocyanate was shown to cause disturbed red blood cell membrane functions, alveolar damage leading to pulmonary oedema (7,10) and immunotoxicity with concomitant disturbances in pulmonary functions (11). With *n*-butyl isocyanate, severe histopathological lesions were observed in rat lungs (12).

In the treatment of cancer patients with fotemustine, haematotoxicity (13) and reversible liver and renal toxicity (3) occurred as toxic side-effects. However, in comparison to other CENUs, such as 1,3-bis(2-chloroethyl)-1-nitrosourea (BCNU), treatment with fotemustine is accompanied with a decreased incidence and severity of side-effects. *In vitro*, it was found that fotemustine, in contrast with BCNU, did not inhibit endogenous enzymes such as GSSG-reductase (14,15), which could be due to the sterical size of the diethyl (1-aminoethyl) phosphonate (DEP) moiety of fotemustine. Data about the molecular mechanisms of the toxic side-effects of fotemustine are scarce and incomplete.

In vitro, fotemustine was only shown to decrease the activity of thioredoxin reductase and ribonucleotide reductase (16). No data are available about the nature of intermediate reactive metabolites of fotemustine, involved in the inactivation of these enzymes. In subcellular rat liver fractions, DEP-isocyanate, a reactive decomposition product of fotemustine, was shown to deplete GSH by conjugation (17). The excretion of GSH-related metabolites in urine of rats treated with fotemustine also points to involvement of GSH in the metabolic inactivation

*Abbreviations: I, [1-(2-oxo imidazolidine-1-yl)ethyl] diethylphosphonate; II, (1-aminoethyl)diethylphosphonate; BCNU, 1,3-bis(2-chloroethyl)-1-nitrosourea; BSA, bovine serum albumin; CCNU, 1-(2-chloroethyl)-3-cyclohexyl-1-nitrosourea; CENU, 2-chloroethyl *N*-nitrosourea; CNC-1, 2-chloroethyl nitrosocarbamoyl alaninemethylamide; CNC-2, 2-chloroethyl nitrosocarbamoyl glycylglycine; CNC-3, 2-chloroethyl nitrosocarbamoyl alanylalanine; CNC-4, 2-chloroethyl nitrosocarbamoylalanine; CNC-5, 2-chloroethyl nitrosocarbamoylglycylglycinemethylamide; DEP-isocyanate, diethyl-ethylphosphonate isocyanate; DEP-SG, diethyl-ethylphosphonate isocyanate glutathione conjugate; DTNB, 5,5-dithiobis(2-nitrobenzoic acid); EDTA, ethylenediaminetetraacetic acid; fotemustine, (diethyl-[1-[3-(2-chloroethyl)-3-nitrosoureydo]-ethyl]phosphonate; FIA, flow injection analysis; γ -GT, γ -glutamyl transpeptidase; GSH, reduced glutathione; GSSG, oxidized glutathione; HECNU, *N*-(2-chloroethyl)-*N'*-(2-hydroxyethyl)-*N*-nitrosourea; HEPES, *N*-(2-hydroxyethyl)-piperazine-*N'*-(2-ethanesulfonic acid); HRP, horseradish peroxidase; LPO, lipid peroxidation; MDA: malondialdehyde; NAC, *N*-acetyl-L-cysteine conjugate; NBT, nitroblue tetrazolium; NEM, *N*-ethyl-maleimide; TBA, thiobarbituric acid; TCA, trichloroacetic acid; TCNU, 1-(2-chloroethyl)-3-[2-(dimethylaminosulfonyl)ethyl]-1-nitrosourea; TEA, triethanolamine; TNB, 5-thio-2-nitrobenzoate.

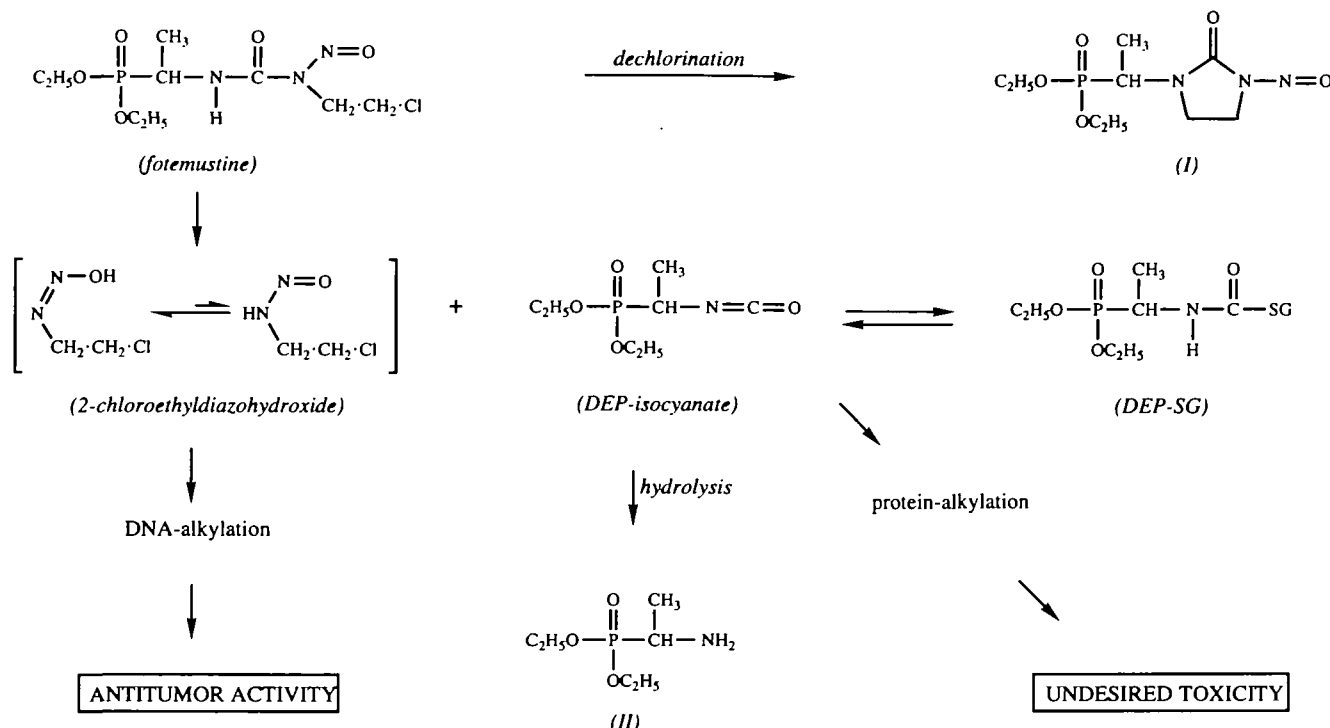


Fig. 1. Schematic overview of the metabolic pathways and mechanisms of action of fotemustine and its primary reactive metabolites; 2-chloroethyl diazohydroxide, DEP-isocyanate and the GSH-conjugate of DEP-isocyanate (DEP-SG). I and II are decomposition products of fotemustine and DEP-isocyanate.

of 2-chloroethyl diazohydroxide, a reactive DNA-alkylating decomposition product of fotemustine (18) (Figure 1). Methyl isocyanate, a reactive decomposition product of caracemide was also shown to conjugate to GSH *in vivo* (19). Furthermore, 2-chloroethyl isocyanate, a reactive decomposition product of BCNU has been demonstrated to form a toxic GSH-conjugate (20). DEP-isocyanate might play a comparable role in the undesired biological effects of fotemustine.

The primary aim of this study is to elucidate possible mechanisms for the cytotoxic effects of fotemustine. For that purpose, the metabolism and the cytotoxicity of fotemustine were first investigated in freshly isolated rat hepatocytes. As parameters for cytotoxicity, lactate dehydrogenase (LDH)-leakage, lipid peroxidation (LPO), depletion of intracellular GSH and formation of GSSG were investigated. The cytotoxicity of DEP-isocyanate and DEP-SG, the GSH-conjugate of DEP-isocyanate (17) were also investigated. Furthermore, the cytotoxicity of six 2-chloroethyl analogues of fotemustine (Figure 2), which are devoid of carbamoylating potency due to intramolecular cyclization and quenching of the generated reactive isocyanate (21), were investigated. The LPO-inducing capacity of fotemustine in rat liver microsomes and the effects of fotemustine on various enzymes in cytosolic rat liver fractions were also studied.

Materials and methods

Chemicals and enzymes

N-ethyl-maleimide (NEM), Triton X-100, bovine serum albumin (BSA) and GSSG reductase (Type III from bakers yeast) were obtained from Sigma (St Louis, USA). Xanthine, xanthine oxidase, collagenase, glucose-6-phosphate, glucose-6-phosphate dehydrogenase, NADH, NADP, sodium pyruvate, GSH (98%) and GSSG (91%) were obtained from Boehringer (Mannheim, Germany). Acetic acid, ammonium acetate, CaCl_2 , DMSO, ethylenediamine-tetraacetic acid (EDTA), ethanol (100%), semicarbazide hydrochloride and triethanolamine (TEA) were obtained from Baker (Deventer, The Netherlands). Sodium azide (NaN_3), 5,5-dithiobis(2-nitrobenzoic acid) (DTNB), glucose,

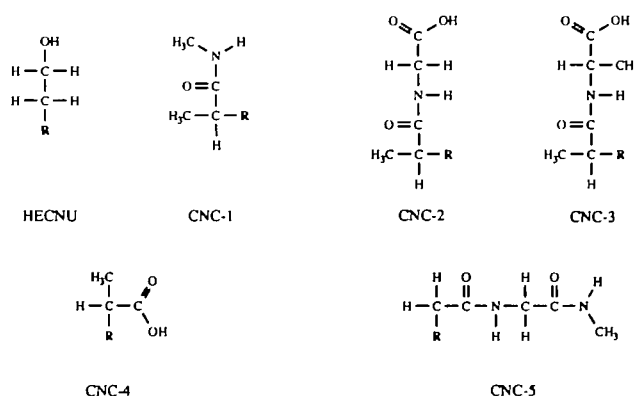


Fig. 2. Chemical structures of 2-chloroethyl derivatives. HECNU, *N*-(2-chloroethyl)-*N'*-(2-hydroxyethyl)-*N*-nitrosourea; CNC-1, 2-chloroethyl nitrosocarbamoyl alaninemethylamide; CNC-2, 2-chloroethyl nitrosocarbamoyl glycylglycine; CNC-3, 2-chloroethyl nitrosocarbamoyl alanylalanine; CNC-4, 2-chloroethyl nitrosocarbamoylalanine; CNC-5, 2-chloroethyl nitrosocarbamoylglycylglycinemethylamide; R, $\text{N}(\text{H})\text{C}(\text{O})\text{N}(\text{NO})\text{CH}_2\text{CH}_2\text{Cl}$.

2,4-pentanedione, pyrazole and trichloroacetic acid (TCA) were obtained from Merck (Darmstadt, Germany). Bromotrifluoromethane and thiobarbituric acid (TBA) was obtained from Aldrich Chemicals (Steinheim, Germany). *N*-(2-hydroxyethyl)piperazine-*N'*-(2-ethanesulfonic acid) (HEPES) was obtained from USB Corporation (Cleveland, Ohio, USA). Trypan blue was obtained from BDH Chemicals LTD (Poole, England). *o*-Dianisidine was obtained from Janssen Chimica (Beerse, Belgium).

Fotemustine (99.8%) was kindly supplied by Servier (Courbevoie, France). Diethyl (1-amidoethyl)phosphonate-glutathione conjugate (DEP-SG) was synthesised from fotemustine and GSH and identified with ^{31}P -NMR and by FAB-MS in glycerol and thioglycerol and by MIKE mass spectrometry as recently described elsewhere (17). Compounds I and II (Figure 1) were synthesized and subsequently characterized with ^{31}P -NMR, ^1H -NMR, EI-MS and CI-MS as described elsewhere (17).

Preparation of cytosolic and microsomal fractions of rat liver. Rat liver cytosol (36.9 mg protein/ml) and microsomes (4.9 mg protein/ml) were prepared by

differential centrifugation of homogenized rat livers as described by Jefcoate (22). The cytosolic and microsomal fractions were stored at -80°C until use.

Incubations with rat liver cytosolic fractions

Rat liver cytosolic fractions (3.69 mg protein/ml) were preincubated with 0 or 1.0 mM fotemustine (1 h, 37°C) and contained 0.3% (v/v) ethanol. After preincubation, superoxide dismutase (SOD), catalase, GSH-peroxidase, GSSG-reductase and total GSH S-transferase activity were investigated in cytosolic rat liver fractions.

Superoxide dismutase activity. Superoxide dismutase (SOD) activity in rat liver cytosol was determined by the inhibition of nitroblue tetrazolium (NBT) reduction by superoxide anion radicals ($\text{O}_2^{\cdot-}$) according to the method of Sazuka *et al.* (23). The reaction mixture (2.9 ml) contained 0.043 M Na_2CO_3 buffer (pH 10.2), 0.1 mM xanthine, 0.1 mM EDTA, 0.05 mg BSA/ml, 0.025 mM NBT and 36 μg rat liver cytosolic protein. After 10 min of preincubation at room temperature, the reaction was started with 75 μl xanthine oxidase (0.05 U/ml). The incubation was carried out for 20 min at 25°C . After addition of 0.2 mM CuCl_2 , the absorbance of the solution was measured spectrophotometrically at 560 nm.

Catalase activity. The catalase activity in rat liver cytosol was measured as described by Sazuka *et al.* (23) by determining the reduction of *o*-dianisidine peroxidation resulting from hydrogen peroxide (H_2O_2) and horseradish peroxidase (HRP). The assay solution contained 120 μg cytosolic rat liver protein/ml and 0.45 mM hydrogen peroxide in a 0.1 M potassium phosphate buffer (pH 7.0). Aliquots of 0.5 ml were removed after 30 and 60 s and added to 2.0 ml of potassium phosphate buffer (50 mM, pH 7.0) containing 0.2 mg *o*-dianisidine/ml, 0.0125 mg HRP/ml and 0.081 mg NaN_3 /ml. After 10 min of incubation at room temperature, 50% (v/v) H_2SO_4 was added to stop the reaction. The absorbance of the reaction medium was measured spectrophotometrically at 530 nm.

GSH-peroxidase activity. The activity of GSH-peroxidase was measured spectrophotometrically at 340 nm by following oxidation of NADPH in cytosolic fractions in the presence of GSH and H_2O_2 as described by Paglia and Valentine (24). The assay solution contained 360 μg cytosolic rat liver protein, 0.3 mM NADPH, 3.8 mM NaN_3 (to inhibit catalase), 5 mM GSH, 70 μM hydrogen peroxide and 2 U/ml yeast GSSG-reductase in a 50 mM potassium phosphate buffer (pH 7.0). The reaction was initiated by the addition of 10 μl of the hydrogen peroxide and measured spectrophotometrically at 340 nm. The final reaction volume of the incubation medium was 2.0 ml.

GSSG-reductase activity. The activity of GSSG-reductase was measured spectrophotometrically at 340 nm by following oxidation of NADPH in cytosolic fractions in the presence of GSSG according to Worthington and Rosemeyer (25). The assay solution contained 3.6 μg cytosolic protein, 0.2 M KCl, 1 mM EDTA, 1 mM GSSG and 0.1 M NADPH in a 0.1 M potassium phosphate buffer (pH 7.0). The reaction was started by the addition of 10 μl cytosolic rat liver fraction and measured spectrophotometrically at 340 nm. The final volume of the incubation medium was 2.0 ml.

GSH S-transferase activity. GSH S-transferase (GST) activity in rat liver cytosol was measured as described by Habig *et al.* (26) using 1-chloro-2,4-dinitrobenzene (CDNB) as substrate. The final reaction mixture (1 ml) contained 0.36 mg cytosolic protein, 1 mM GSH and 1 mM CDNB in potassium phosphate buffer (0.1 M, pH 6.5). The reaction was started by the addition of 10 μl of 100 times diluted cytosolic rat liver fraction and the increase in absorbance was measured spectrophotometrically at 340 nm.

Incubations with rat liver microsomal fractions

Lipid peroxidation. Rat liver microsomal fractions (0.49 mg/ml protein) were preincubated with 0 or 1.0 mM fotemustine (1 h, 37°C) which contained 0.3% (v/v) ethanol. Before and after preincubation, LPO was investigated in the microsomal fractions by measuring malondialdehyde production with thiobarbituric acid (TBA) as described by Haenen *et al.* (27). All the incubation mixtures were buffered with Tris-HCl (50 mM; pH 7.4) and contained semicarbazide hydrochloride (3 mM), MgCl_2 (3 mM), NADP (0.3 mM), glucose-6-phosphate (3 mM) and glucose-6-phosphate dehydrogenase (0.7 U/ml). A 0.2 ml aliquot of the microsomal incubation mixture was added to a 0.375% (w/v) TBA, 15% (w/v) TCA in 0.25 M HCl solution. After heating for 30 min at 80°C and centrifugation for 15 min at 4°C , the absorbance at 535 nm versus 600 nm in the supernatant was determined spectrophotometrically.

Isolation of rat hepatocytes

Hepatocytes were isolated from fasted male Wistar rats (200–220 g; Harland, Zeist, The Netherlands) by collagenase perfusion of the liver as described previously by Nagelkerke *et al.* (28). The preperfusion and perfusion solutions were buffered at pH 7.4 and pH 7.6, respectively, with 10 mM HEPES. The total time of the perfusion was ~15–20 min. Aliquots of the freshly isolated

hepatocytes were immediately counted with a hemacytometer in 0.4% trypan blue solution containing 0.9% NaCl. The viability of the cells isolated by this method was always $>90\%$.

Incubations with rat hepatocytes

The freshly isolated rat hepatocytes (10^6 cells/ml) were incubated with (i) 800 μM fotemustine, (ii) 0, 10, 20, 50, 100, 200 or 500 μM fotemustine, (iii) *N*-(2-chloroethyl)-*N'*-(2-hydroxyethyl)-*N*-nitrosourea (HECNU), 2-chloroethyl nitrosocarbamoyl alaninemethylamide (CNC-1), 2-chloroethyl nitrosocarbamoyl glycylglycine (CNC-2), 2-chloroethyl nitrosocarbamoyl alanylalanine (CNC-3), 2-chloroethyl nitrosocarbamoyl alanine (CNC-4) or 2-chloroethyl nitrosocarbamoyl glycylglycinemethylamide (CNC-5), BCNU or fotemustine and with (iv) 500 μM fotemustine or 500 μM DEP-SG.

At various timepoints after starting the respective incubations, samples were taken for the determination of LDH-leakage, LPO and the concentrations of GSH and GSSG. The total volume of all the incubation mixtures was 7 ml. In order to dissolve the various compounds, the incubation mixtures contained a minor concentration of ethanol (in all cases $<0.3\%$ (v/v)). All the incubations were repeated at least three times at different days. For all the investigated parameters, analysis was performed in duplicate.

Cytotoxicity assays

LDH-leakage. Samples of 0.5 ml were taken from the hepatocyte incubations (10^6 cells/ml) and centrifuged (50 g; 4 min; 4°C). LDH-leakage was determined in the supernatant fraction via NADH oxidation in the presence of sodium pyruvate as previously described by van de Straat *et al.* (29). The final reaction mixture contained 0.2 mM NADH and 0.5 mM sodium pyruvate in 50 mM triethanolamine (TEA) buffer (pH 7.4). The enzymatic reaction was initiated by the addition of 20 μl of the supernatant.

Lipid peroxidation. Samples of 0.5 ml were taken from the hepatocyte incubations (10^6 cells/ml) and malondialdehyde (MDA) was determined as a parameter for lipid peroxidation (LPO) as described above according to Haenen *et al.* (27).

GSH and GSSG concentrations. Samples of 0.5 ml were taken from the hepatocyte incubations (10^6 cells/ml) and centrifuged (50 g; 4 min; 4°C). Intracellular concentrations of GSH and GSSG were determined in the resuspended cell pellets using the flow injection analysis (FIA) method previously described by Redegeld *et al.* (30). Briefly, total glutathione (GSH plus GSSG) concentrations were determined via an enzymatic recycling reaction of GSH in a chromogenic reaction with 5,5-dithiobis(2-nitrobenzoic acid) (DTNB), finally leading to the formation of 5-thio-2-nitrobenzoate (TNB) with an absorption maximum at 412 nm (30). Oxidized glutathione (GSSG) was determined analogously except that the reduced GSH was first trapped through reaction with an excess *N*-ethylmaleimide (NEM). Extracellular GSSG concentrations were determined in the supernatant after addition of 8.6 μl of 70% HClO_4 , as previously described (30).

Metabolism of fotemustine and DEP-SG

Incubations of the freshly isolated rat hepatocytes (10^6 cells/ml, buffered with HEPES (10 ml, pH 7.4)) with 2 mM fotemustine or 2 mM DEP-SG were followed with time by ^{31}P -NMR. Relatively high concentrations of fotemustine and DEP-SG (2 mM) were chosen to investigate their metabolism, because the detection limits of both compounds in hepatocytes are ~250 μM . The incubations contained 1.5% albumin. Control incubations of fotemustine were performed (2 mM) in HEPES buffer (10 mM, pH 7.4) without hepatocytes and in the absence or the presence of albumin (1.5%). Samples of 4.8 ml were taken from the incubation media at 0 and 180 min and measured immediately with ^{31}P -NMR.

Phosphorus NMR

Proton-decoupled ^{31}P -NMR measurements were performed on a Bruker MSL 280 system (162.0 MHz, 10 mm dual, ^{31}P - ^{19}F probe). The apparatus collected 20 scans/min over time periods of 5 min during the first hour of the incubations and over time periods of 30 min thereafter. The maximal resolution of ^{31}P -NMR signals in freshly isolated rat hepatocytes was 0.05 p.p.m. Chemical shifts may deviate by 0.08 p.p.m., due to small differences in pH (± 0.05) and in composition of the hepatocyte solutions. The ^{31}P -NMR chemical shifts are expressed in p.p.m., relative to the chemical shift of 85% H_3PO_4 (0 p.p.m.).

Data analyses

The experimental results were evaluated statistically using the Student's *t*-test and were considered significant if $P < 0.05$ in at least three different incubations performed on different days.

Results

Metabolism of fotemustine and DEP-SG in rat hepatocytes

Figure 3 shows ^{31}P -NMR spectra in freshly isolated rat hepatocytes either incubated with 2 mM fotemustine or with

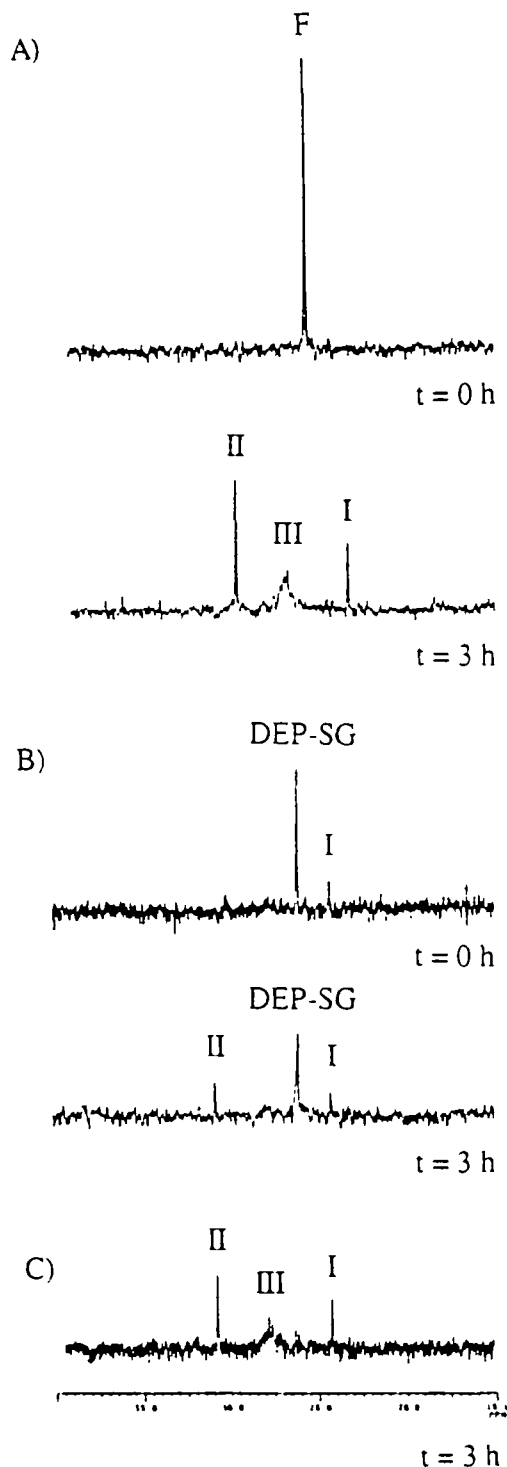


Fig. 3. ³¹P-NMR spectra of freshly isolated rat hepatocytes, 0 and 3 h after starting incubations with 2 mM fotemustine (A) or 2 mM DEP-SG (B) and ³¹P-NMR spectra of an incubation mixtures of 2 mM fotemustine in HEPES buffer in the presence of 1.5% albumin, after 3 h of incubation (C).

2 mM DEP-SG. After 3 h of incubation, fotemustine was converted completely in these hepatocytes. Approximately 45% of fotemustine (*s*, δ = 26.1 p.p.m.) converted into compound II (*s*, δ = 30.3 p.p.m.) (Figure 3A), previously identified as a hydrolytic decomposition product of DEP-isocyanate (17). Approximately 20% of fotemustine decomposed into compound I (*s*, δ = 24.0 p.p.m.), the dechlorination

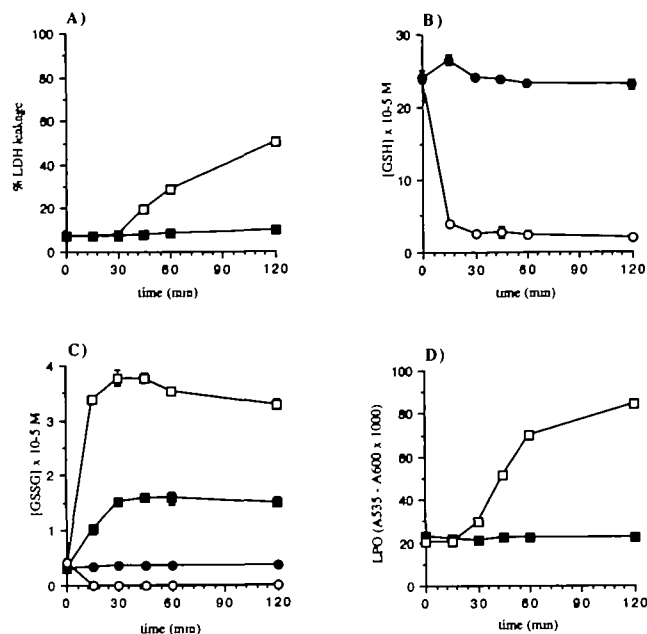


Fig. 4. LDH-leakage (A), intracellular GSH-levels (B), intra- plus extracellular GSSG-levels (C) and LPO (D) in freshly isolated rat hepatocytes upon incubation with 0 and 800 μM fotemustine. ■, Control (extracellular); □, 800 μM fotemustine (extracellular); ○, control (intracellular); ●, 800 μM fotemustine (intracellular).

product of fotemustine (17). Moreover, ~35% of fotemustine converted into a variety of products (III), visible between 27.3 and 28.1 p.p.m. These products were also found to be formed in incubations of fotemustine in HEPES buffer and albumin (1.5%) without hepatocytes (Figure 3C). ³¹P-NMR spectra of the conversion of fotemustine in HEPES buffer without albumine and hepatocytes were completely similar to the ³¹P-NMR spectra as shown recently (17).

In incubations in buffer without albumin, the products between 27.3 and 28.1 p.p.m. (III) (Figure 3C) were not formed. During 3 h of incubation in rat hepatocytes, ~30% of DEP-SG (*d*, δ = 26.2 p.p.m.), the GSH-conjugate of DEP-isocyanate, converted into compound II (*s*, δ = 30.7 p.p.m.) (Figure 3B), which was recently identified as a hydrolytic decomposition product of DEP-isocyanate (17). Approximately 60% of the original DEP-SG remained stable in the hepatocytes during 3 h of incubation. The remaining 10% of DEP-SG was not recovered after 3 h of incubation. A minor quantity of compound I (*s*, δ = 24.2 p.p.m.), a byproduct in the synthesis of DEP-SG (17), was visible during the whole time course of the incubation (Figure 3B).

Extent and time-dependency of cytotoxicity of fotemustine

To find out whether fotemustine was cytotoxic to freshly isolated rat hepatocytes, the extent of LDH-leakage, lipid peroxidation (LPO), depletion of GSH and the formation of intra- and extracellular GSSG were first investigated upon addition of a relatively high concentration of fotemustine. Furthermore, the time dependency of the various toxicity parameters was investigated.

Figure 4 shows the LDH-leakage (Figure 4A), intracellular GSH-levels (Figure 4B), intracellular and extracellular GSSG-levels (Figure 4C) and LPO (Figure 4D) in freshly isolated rat hepatocytes incubated with 800 μM fotemustine. The GSH-level decreased rapidly and almost completely upon addition of fotemustine (Figure 4B). The intracellular GSSG-levels

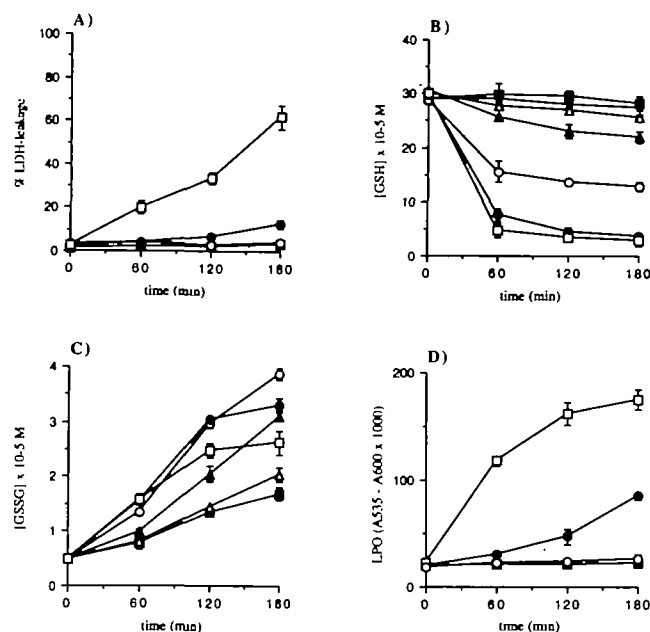


Fig. 5. LDH-leakage (A), intracellular GSH-levels (B), extracellular GSSG-levels (C) and LPO (D) upon incubation of freshly isolated rat hepatocytes with 0, 10, 20, 50, 100, 200 and 500 μM fotemustine. LDH-leakage in incubations with 10, 20 and 50 μM fotemustine are not shown because data were not significantly different from the controls. GSSG formation in the incubation with 10 μM fotemustine is not significantly different from the controls. LPO in the incubations with 10, 20 and 50 μM fotemustine was not significantly different from the controls. ■, Control; ×, 10 μM fotemustine; △, 20 μM fotemustine; ▲, 50 μM fotemustine; ○, 100 μM fotemustine; ●, 200 μM fotemustine; □, 500 μM fotemustine.

decreased rapidly to non-detectable concentrations ($<3 \mu\text{M}$) (Figure 4C), while the extracellular GSSG-levels increased rapidly and significantly (Figure 4C). In subsequent experiments, only the extracellular GSSG concentrations were measured therefore. After 30 min of incubation, the extracellular levels of GSSG remained relatively stable (Figure 4C). Significant LPO, measured as TBA-reactive material, was observed after 30 min of incubation of the hepatocytes with 800 μM fotemustine (Figure 4D). LPO seemed to precede the fotemustine-induced LDH-leakage, which was observed only 45 min after starting the incubation of the hepatocytes with fotemustine (Figure 4A and 4D). During the remaining time course of the incubations both LPO (Figure 4D) and LDH-leakage (Figure 4A) increased further.

Concentration dependency of the cytotoxicity of fotemustine

The concentration and time versus effect relationships of fotemustine-induced LDH-leakage, LPO, depletion of GSH and formation of GSSG were subsequently investigated in the freshly isolated hepatocytes. Figure 5 shows the time course of LDH-leakage (Figure 5A), intracellular GSH-levels (Figure 5B), extracellular GSSG-levels (Figure 5C) and LPO (Figure 5D) in rat hepatocytes incubated with different concentrations of fotemustine. A concentration-dependent decrease of intracellular GSH-levels was observed up to 180 min (Figure 5B). A concentration of 50 μM fotemustine caused a significant decrease and concentrations of 200 μM and 500 μM fotemustine caused a rapid and nearly complete exhaustion of the GSH-levels in rat hepatocytes (Figure 5B). Below a fotemustine concentration of 100 μM , a concentration- and time-dependent increase of extracellular GSSG-levels was observed (Figure 5C). Above 100 μM fotemustine, extracellular GSSG-levels

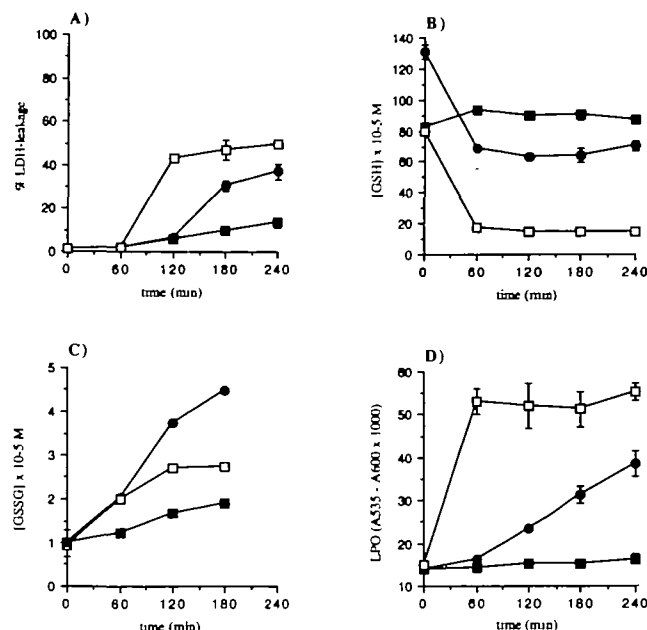


Fig. 6. LDH-leakage (A), intracellular GSH-levels (B), extracellular GSSG-levels (C) and LPO (D) upon incubation of freshly isolated rat hepatocytes with 500 μM fotemustine or 500 μM DEP-SG. ■, Control; □, 500 μM fotemustine; ●, 500 μM DEP-SG.

increased only up to 120 min and remarkably the extent of the increase declined with increasing concentrations of fotemustine (Figure 5C).

No LDH-leakage nor LPO were observed upon treatment of the hepatocytes with fotemustine up to 100 μM (Figure 5A and 5D). Concentration dependent LPO and LDH-leakage were observed upon treatment of the hepatocytes with concentrations of fotemustine $>100 \mu\text{M}$ (Figure 5A and 5D).

Cytotoxicity of DEP-SG

Figure 6 shows the time-dependency of LDH-leakage (Figure 6A), intracellular GSH-levels (Figure 6B), extracellular GSSG-levels (Figure 6C) and LPO (Figure 6D) in rat hepatocytes incubated either with 500 μM DEP-SG, the GSH-conjugate of DEP-isocyanate, or with 500 μM fotemustine. At this concentration, fotemustine induced LDH-leakage, LPO and a depletion of intracellular GSH, while the extracellular GSSG-levels in rat hepatocytes were increased, similar to the previous observations (Figures 4 and 5). DEP-SG was less cytotoxic, when measured as LDH-leakage and LPO. Nevertheless, 500 μM DEP-SG caused a significant LDH-leakage and LPO in the hepatocytes. LPO was already statistically significant after 2 h of incubation with 500 μM DEP-SG (Figure 6D), the LDH-leakage was significant only after 3 h of incubation, however (Figure 6A). Thus, the LPO caused both by DEP-SG and by fotemustine preceded the corresponding LDH-leakage. A concentration of 500 μM DEP-SG also caused a significant decrease of the intracellular GSH-levels in the rat hepatocytes. Remarkably, extracellular GSSG-levels increased to a larger extent upon incubation of the hepatocytes with DEP-SG when compared to an equimolar concentration of fotemustine (Figure 6C).

Administration of 250 μM DEP-SG to the hepatocytes did not cause LDH-leakage nor LPO, however, it did cause a significant decrease of the intracellular GSH-levels and an increase of the extracellular GSSG-levels (data not shown).

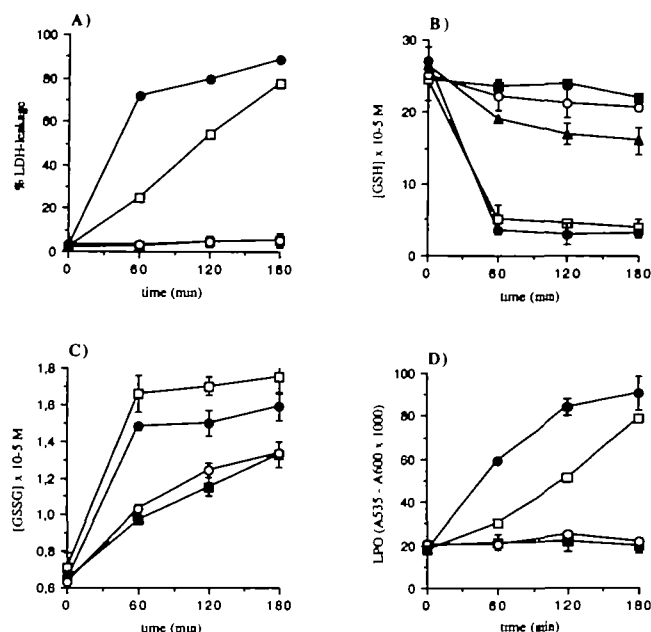


Fig. 7. LDH-leakage (A), intracellular GSH-levels (B), extracellular GSSG-levels (C) and LPO (D) upon incubation of freshly isolated rat hepatocytes with 1 mM fotemustine, BCNU and the 2-chloroethyl analogues HECNU and CNC-1, CNC-2, CNC-3, CNC-4 and CNC-5. The LDH-leakage, LPO and GSSG-formation in incubations with HECNU and CNC-1, CNC-2, CNC-3, CNC-4 and CNC-5 was not significantly different from the controls. Therefore, only LDH-leakage, LPO and GSSG-formation upon incubation with 1 mM HECNU is shown. The time-course of the GSH-levels upon incubation with HECNU and CNC-1, CNC-2, CNC-3 and CNC-5 was not significantly different. Therefore, only the GSH-levels upon incubation with HECNU and CNC-4 are shown. ■, Control; □, 1 mM fotemustine; ●, 1 mM BCNU; ○, 1 mM HECNU; ▲, 1 mM CNC-4.

Cytotoxicity of BCNU and 2-chloroethyl analogues of fotemustine

Figure 7 shows the time-dependency of LDH-leakage (Figure 7A), intracellular GSH-levels (Figure 7B), extracellular GSSG-levels (Figure 7C) and LPO (Figure 7D) in freshly isolated rat hepatocytes incubated with HECNU and CNC-1, CNC-2, CNC-3, CNC-4, CNC-5, BCNU and fotemustine at concentrations of 1 mM. Similar to previous observations (Figures 4, 5 and 6), fotemustine caused LDH-leakage, LPO, GSH-depletion and GSSG-formation. In the case of BCNU, the extent of LDH-leakage and LPO were faster and higher than with fotemustine, however, no significant differences were observed in GSH-depletion (Figure 7A, 7B and 7D). The increase of extracellular GSSG upon incubation with BCNU was significantly lower than with fotemustine (Figure 7C). None of the 2-chloroethyl analogues of fotemustine caused any significant LDH-leakage, LPO or GSSG-formation. Except for CNC-4, none of the 2-chloroethyl analogues significantly decreased GSH-levels.

Effects of fotemustine on antioxidant enzymes in cytosolic rat liver fractions

Table I shows the effects of fotemustine on SOD, catalase, GSH-peroxidase, GSSG-reductase and GSH S-transferases, all being cytosolic enzymes directly or indirectly involved in cytoprotective antioxidant processes. No statistically significant effects were observed of fotemustine on SOD, catalase, GSH-peroxidase and GSSG-reductase nor on GSH S-transferases in cytosolic rat liver fractions (Table I).

Table I. Effects of fotemustine on SOD, catalase, GSH-peroxidase, GSSG-reductase and GSH S-transferases in non-induced cytosolic rat liver fractions after 1 h of preincubation

Enzyme	Fotemustine (mM)	Enzyme activity (U/mg cytosolic protein)
SOD	0	0.10 ± 0.01
	1	0.10 ± 0.01
catalase	0	10.2 ± 0.71
	1	11.1 ± 0.57
GSH-peroxidase	0	0.83 ± 0.02
	1	0.84 ± 0.03
GSSG-reductase	0	19.1 ± 0.9
	1	18.0 ± 1.4
GSH S-transferase	0	2.32 ± 0.06
	1	2.55 ± 0.15

Table II. LPO, measured as formation of TBA-reactive products, in rat liver microsomal fractions upon 1 h of incubation with fotemustine

Fotemustine (mM)	LPO (ΔA _{535nm-600nm} × 1000)
0	0.08 ± 0.01
1	0.08 ± 0.00

LPO is expressed as ΔA_{535nm-600nm} × 1000 of TBA-reactive material and corrected for the 0 h background values.

Fotemustine-induced LPO in microsomal rat liver fractions

The fotemustine-induced LPO in rat liver microsomal fractions, measured as formation of TBA-reactive material, was also investigated. No direct LPO was observed by fotemustine in rat liver microsomal fractions measured (Table II). Bromotrachloromethane, which was used as a positive control compound for the experimental procedures, caused extensive LPO in rat microsomes (data not shown).

Discussion

Therapy of cancer patients with fotemustine is sometimes hampered by haemato- and lung toxicity (13) and by mild but reversible renal- and liver toxicity (3). As yet, almost nothing is known about the mechanisms of these side-effects of fotemustine. This study is therefore aiming at the elucidation of potential molecular mechanisms underlying the cytotoxic properties of fotemustine.

Metabolism of fotemustine and DEP-SG in rat hepatocytes

The metabolism of fotemustine and DEP-SG, the GSH-conjugate of DEP-isocyanate, was first investigated in hepatocytes to find out whether the metabolic behaviour of both compounds might explain their cytotoxicity. Fotemustine was found to be metabolized in compounds I, II and III (Figures 1 and 3). Its metabolic profile was qualitatively comparable to that observed earlier, *in vitro*, in HEPES buffer and rat liver-S₉ fractions (17) and *in vivo*, in rats (Brakenhoff, J.P.G. *et al.*, in preparation). In the hepatocytes, however, a much smaller fraction of fotemustine decomposed into compound II, a hydrolytic decomposition product of DEP-isocyanate (17). The latter observation is likely due to albumin as can be deduced from the ³¹P-NMR spectrum of a control incubation (Figure 3C). Reversible exchange of DEP-isocyanate with nucleophiles present in albumin leads to continuous regeneration of DEP-isocyanate and formation of compound II. Reversible reactivity

of iso(thio)cyanates has been shown to occur in the case of GSH-conjugates of benzyl- and allyl isothiocyanate (31) and of methyl isocyanate conjugated to the amino group in the terminal valine residue of haemoglobin (32) and thiols or amines in other proteins (33).

The formation of compound II in the present incubations with DEP-SG (Figure 3), indicates that DEP-isocyanate must have been formed in the incubations with DEP-SG. Therefore, DEP-isocyanate can be formed both from fotemustine and from DEP-SG as shown in Figure 1. In freshly isolated rat hepatocytes, DEP-SG was much less stable than in HEPES buffer at the same temperature (this study, 17). This medium-dependent difference in stability of DEP-SG can probably be explained by the formation of adducts between DEP-isocyanate and albumin or other proteins in hepatocytes. Approximately 10% of the original DEP-SG could not be recovered in the hepatocytes with a ^{31}P -NMR spectrum taken after 3 h of incubation. This fraction of DEP-SG is probably converted into non-identified adducts to albumin or other proteins.

Time-dependency of the cytotoxicity of fotemustine

Firstly, the cytotoxic effects of a relatively high concentration of fotemustine were investigated in rat hepatocytes (Figure 4). A concentration of 800 μM of fotemustine caused a significant LDH-leakage 45 min after starting the incubations. The LDH-leakage was preceded by LPO, which was measured as TBA-reactive material and observed 30 min after starting the incubations. The fotemustine-induced LPO was in turn preceded by extensive GSH-depletion, an extensive decrease of intracellular GSSG and an increase of extracellular GSSG-levels. The effects of fotemustine on GSH- and GSSG-levels were already measurable 15 min after starting the incubations. The rapid and extensive decrease of the intracellular GSH-levels supports the ability of fotemustine to pass the cellular membrane rapidly.

Chemically induced LPO in rat hepatocytes can be a cause as well as a consequence of cell death (34). In the case of fotemustine, LPO preceded LDH-leakage suggesting a causal relationship with cell death (27). Extensive depletion of intracellular GSH is known to enhance LPO because of a hampered cellular protective antioxidant capacity against radical damage (27,35). In the metabolism of fotemustine no free radicals are formed (17,18). However, endogenous free radicals formed after depletion of intracellular GSH (36) might also contribute to the generation of LPO. Depletion of GSH by fotemustine is most likely caused by DEP-isocyanate, a reactive decomposition product of fotemustine (17). In incubations of fotemustine with hepatocytes, DEP-isocyanate is indeed formed as can be deduced from the formation of compound II, a known hydrolytic decomposition product of DEP-isocyanate (17,18) (Figure 3).

Concentration-dependency of the cytotoxicity of fotemustine

Fotemustine concentration versus effect relationships were also investigated in the hepatocytes. Upon exposure of hepatocytes to fotemustine in concentrations $<200\text{ }\mu\text{M}$, no LDH-leakage nor LPO were observed, despite the fact that a significant concentration-dependent decrease in GSH-levels and increase in GSSG-levels were observed. Obviously, the cellular protection against the cytotoxicity of fotemustine is sufficient as long as sufficient GSH is present. Fotemustine concentrations $\geq 200\text{ }\mu\text{M}$ were cytotoxic to the rat hepatocytes. GSH is known to be the major cellular thiol-compound protecting proteins from covalent binding to reactive intermediates and from

oxidative damage (37,38). Covalent binding of reactive intermediates to protein-thiols in calcium translocases located in the plasma membrane, microsomes or mitochondria is known to lead to a disturbed cellular calcium homeostasis (38–40). Depletion of intracellular calcium is known to cause an increase of cellular peroxides, ultimately leading to LPO (41). In principle, LPO might also be due to inhibitory effects on thioredoxin reductase, an enzyme involved in various anti-oxidant processes (16).

The GSH-depletion observed upon incubation of rat hepatocytes with fotemustine can be explained by conjugation of GSH to DEP-isocyanate. Other metabolic pathways of DEP-isocyanate apparently occur only after complete depletion of GSH. The observed GSH-depletion, however, might also be explained by oxidation of GSH to GSSG, chemically or as a result of GSH-peroxidase- or GSSG-reductase-mediated reduction of hydroperoxides (42). GSSG is known to be efficiently transported out of liver cells by an ATP-dependent translocase and is therefore measured extracellularly (39).

Cytotoxicity of DEP-SG

In order to investigate the possible role of the reactive DEP-isocyanate in the cytotoxicity induced by fotemustine, the various cytotoxicity parameters were also determined in hepatocytes incubated with synthetic DEP-SG, the GSH-conjugate of DEP-isocyanate and a precursor of DEP-isocyanate.

The cytotoxicity of DEP-SG was found to be significantly lower than that of fotemustine (Figure 6). The fact that in the case of DEP-SG lower amounts of compound II, a hydrolysis product of DEP-isocyanate, were detected than in the case of fotemustine, suggests that lower concentrations of DEP-isocyanate have been present in the incubations with DEP-SG. This might explain the lower toxicity of DEP-SG when compared to fotemustine. The observed cytotoxicity of DEP-SG supports our earlier suggestion that GSH-conjugation of DEP-isocyanate is only a temporary mechanism of protection against the toxicity of fotemustine due to apparent reversibility of the GSH-conjugation reaction with DEP-isocyanate (17).

In incubation mixtures with DEP-SG, the initial intracellular GSH-level was found to be significantly higher than in incubation mixtures with fotemustine. However, control experiments revealed that with the FIA method applied, GSH also conjugated to DEP-isocyanate and/or the GSH liberated from DEP-SG could be measured (data not shown). As a consequence, the decrease of intracellular GSH-levels observed in incubations with fotemustine and DEP-SG is essentially reflecting the decrease of the sum of intracellular GSH and intracellular DEP-SG or GSH derived from DEP-SG. This observation supports the suggestion that DEP-SG, containing a lipophilic diethyl (1-amidoethyl) phosphonate side chain, rapidly passes cellular membranes (43). GSH-conjugates are known to pass cellular membranes via different mechanisms of active transport (44). Decreasing amounts of GSH in incubations with DEP-SG or fotemustine (Figure 6B) can be explained by oxidation into GSSG or by further metabolism of DEP-SG. For example, GSH-conjugates are known to be cleaved by γ -glutamyl transpeptidase (γ -GT), a hydrolytic enzyme located mainly in the hepatic cell membranes (44).

Remarkably, in hepatocytes incubated with DEP-SG, the increase of GSSG-levels was higher than in similar incubations with fotemustine. The latter is probably due to an almost complete exhaustion of GSH, which occurred rapidly upon

incubation with fotemustine but not upon incubation with DEP-SG (Figure 6B). GSH-conjugates of both methyl and 2-chloroethylisocyanate are potent inhibitors of GSSG-reductase, which might also lead to increased levels of GSSG (45,46). DEP-SG-induced formation of GSSG, however, is difficult to explain by this phenomenon because DEP-isocyanate, its reactive decomposition product, was shown to be devoid of inhibiting properties towards GSSG-reductase (*this study*).

Cytotoxicity of BCNU and 2-chloroethyl analogues of fotemustine

In the present study, BCNU appeared to be more cytotoxic than fotemustine, probably because of a higher reactivity of 2-chloroethylisocyanate when compared to that of DEP-isocyanate. GSSG formation, however, was significantly lower in incubations with BCNU than with fotemustine. Because the inhibitory activity of BCNU towards GSSG-reductase is higher when compared to that of fotemustine (2), a higher formation of GSSG was expected in the case of BCNU. The fact that the reverse was observed may be explained by a more rapid and complete depletion of GSH in incubations with BCNU.

The present study has shown that only fotemustine and BCNU, which are both known to form reactive isocyanates (17,21,47), cause GSH-depletion, GSSG-formation and cytotoxicity in hepatocytes. In contrast, the 2-chloroethyl analogues of fotemustine, HECNU and CNC-1, CNC-2, CNC-3 and CNC-5, which have no carbamoylating potency as a result of intramolecular quenching of the reactive isocyanate (21), were found not to be cytotoxic in the present study. This confirms our suggestion that reactive isocyanates are mainly responsible for the observed GSH-depletion and cytotoxicity with CENUs in rat hepatocytes. The fact that CNC-4, in contrast to the other investigated 2-chloroethyl analogues, decreased the intracellular GSH-levels in hepatocytes is reasonable because the isocyanate moiety of CNC-4 cannot be inactivated by intra-molecular amide formation (21). The reactive 2-chloroethyldiazohydroxides which can be formed from fotemustine, BCNU and from HECNU and CNC-1–CNC-5 are apparently inferior in this regard. Studies on the involvement of 2-chloroethyldiazohydroxides in undesired effects are very scarce. Only the bone-marrow toxicity upon therapy with CENUs has been related to 2-chloroethylation of endogenous nucleophilic sites (48). Relationships between the carbamoylating capacity of CENUs and toxic side-effects, however, have been well documented (48–50). The difference in severity of toxic side-effects of BCNU and HECNU was suggested to be caused by the difference in carbamoylating capacity of both CENUs (14).

Effects of fotemustine in rat liver cytosolic and microsomal fractions

To find out whether fotemustine or its reactive decomposition product DEP-isocyanate cause peroxidation of cellular membranes, we investigated LPO as well as possible inhibitory effects of both compounds on enzymes involved in antioxidant processes.

In contrast to the observations in hepatocytes, in rat liver microsomes no direct LPO was observed with fotemustine. Obviously, as with other CENUs, no radicals are formed during metabolism or chemical decomposition of fotemustine. Furthermore, no inhibitory effects of fotemustine were observed on SOD, catalase, GSH-peroxidase and GSSG-reductase nor on GSH S-transferases in cytosolic rat liver fractions. This suggests that the LPO observed upon incubation

of hepatocytes with fotemustine is not likely explained by inhibitory effects of fotemustine on the above-mentioned antioxidant enzymes. Inhibitory effects on GSSG-reductase have been described for BCNU (47,51) and other CENUs such as chlorozotocin, CCNU and TCNU (52). This inhibiting activity was shown to be related to the carbamoylating properties of their reactive isocyanate decomposition products (52). In line with the present study, Boutin *et al.* (15) found that fotemustine did not inhibit GSSG-reductase. It has been suggested that this is due to the size of the diethyl (1-amidoethyl) phosphonate (DEP)-moiety of fotemustine. BCNU and HECNU were previously reported to inhibit GSH S-transferase activity in bone marrow but not in other tissues (48). No inhibitory effects of CENUs on GSH-peroxidase, SOD or catalase are known.

The observed absence of fotemustine-induced LPO in rat liver microsomes and the absence of inhibitory effects of fotemustine on cytosolic antioxidant enzymes suggest that the fotemustine-induced LPO occurs at the mitochondrial level. In line with this suggestion, methylisocyanate was recently shown to cause LPO in rat liver mitochondria (53), while 2-chloroethylisocyanate, a reactive decomposition product of BCNU, was shown to cause LPO in rat hepatocytes by depletion of mitochondrial GSH (54).

In summary, fotemustine was found to cause concentration- and time-dependent cytotoxic effects in rat hepatocytes. GSH-depletion and GSSG-formation were first observed, subsequently LPO and finally cell death, measured as LDH-leakage. A number of 2-chloroethyl analogues of fotemustine, which in contrast to fotemustine, have no carbamoylating capacity due to intramolecular quenching of their reactive isocyanate decomposition products, were not toxic to rat hepatocytes. This supports the suggestion that the toxicity of fotemustine is caused by DEP-isocyanate. Fotemustine did not induce LPO in rat liver microsomes, nor did fotemustine affect the rat liver cytosolic antioxidant enzymes SOD, catalase, GSH-peroxidase, GSSG-reductase and GSH S-transferases. These observations support the suggestion that the fotemustine-induced LPO in hepatocytes is most likely a result of rapid and extensive depletion of GSH by DEP-isocyanate. GSH-conjugation of DEP-isocyanate is apparently not an effective mechanism of detoxification because DEP-SG, the GSH-conjugate of DEP-isocyanate was also toxic to the rat hepatocytes.

GSH-depletion by DEP-isocyanate and concomitant oxidative cell damage may also play a role in the toxic side-effects observed in patients, such as haemato, liver and renal toxicity (Brakenhoff, J.P.G. *et al.* the present study can be helpful in explaining these toxic side effects as well as in the design of chemoprotective tools (55).

Acknowledgements

The authors wish to thank Dr F.J.J.de Kanter for valuable ³¹P-NMR measurements and Dr. B.L.M van Baar for his efforts to identify synthetic DEP-SG with FAB-MS and with MIKE mass spectrometry. We wish to thank Professor G.Eisenbrand of the Department of Food Chemistry and Environmental Toxicology, University of Kaiserslautern, Germany for helpful discussion and for his kindness in supplying us with all the 2-chloroethyl analogues of fotemustine.

References

1. Fischel, J.L., Formento, P. and Etienne, M.C. (1990) *In vitro* chemosensitivity testing of fotemustine (S10036), a new antitumor nitrosourea. *Cancer Chem. Pharmacol.*, **25**, 727–729.

2. Bizzari, J.-P. and Deloffre, P. (1988) Pharmacocinetique clinique des nitrosourees. *Bull. Cancer*, **75**, 813–818.
3. Jacquillat, C., Khayat, D., Banzet, P. et al. (1990) Final report of the french multicenter phase II study of the nitrosourea fotemustine in 153 evaluable patients with disseminated malignant melanoma including patients with cerebral metastasis. *Cancer*, **66**, 1873–1878.
4. Patterson, R., Nugent, K.M., Harris, K.E. and Eberle, M.E. (1990) Immunologic hemorrhagic pneumonia caused by isocyanates. *Am. Rev. Resp. Dis.*, **141**, 226–230.
5. Kramer, R.A., Boyd, M.R. and Dees, J.H. (1986) Comparative nephrotoxicity of 1-(2-chloroethyl)-3-(trans-4-methylcyclohexyl)-1-nitrosourea (MeCCNU) and chlorozotocin: functional-structural correlations in the Fischer 344 rat. *Toxicol. Appl. Pharmacol.*, **82**, 540–550.
6. Babson, J., Reed, D. J. and Sinkey, M.A. (1977) Active site specific inactivation of chymotrypsin by cyclohexyl isocyanate formed during degradation of the carcinostatic 1-(2-chloroethyl)-1-nitrosourea. *Biochemistry*, **16**, 1584–1589.
7. Jeevaatnam, K. and Vaidyanathan, C.S. (1992) Acute toxicity of methyl isocyanate in rabbit. *in vitro* and *in vivo* effects on rabbit erythrocyte membrane. *Arch. Environ. Toxicol.*, **22**, 300–304.
8. Babson, J.R. and Reed, D.J. (1978) Inactivation of glutathione reductase by 2-chloroethylnitrosourea-derived isocyanates. *Biochem. Biophys. Res. Commun.*, **83**, 754–762.
9. Lee, M.-S. (1992) Oxidative conversion by rat liver microsomes of 2-naphthyl isothiocyanate to 2-naphthyl isocyanate, a genotoxicant. *Chem. Res. Toxicol.*, **5**, 791–796.
10. Nemery, B., Dinsdale, D., Sparrow, S. and Ray, D.E. (1985) Effects of methyl isocyanate on the respiratory tract of rats. *Br. J. Ind. Med.*, **42**, 799–805.
11. Karol, M.H. and Jin, R. (1991) Mechanisms of immunotoxicity to isocyanates. *Chem. Res. Toxicol.*, **4**, 503–509.
12. Pauluhn, J. and Eben, A. (1992) Altered lung function in rats after subacute exposure to n-butyl isocyanate. *Arch. Toxicol.*, **66**, 118–125.
13. Gerard, B., Aamdal, S., Lee, S.-M., Leyvraz, S., Lucas, C., D'Incalci, M. and Bizzari, J.P. (1993) Activity and unexpected lung toxicity of the sequential administration of two alkylating agents-dacarbazine and fotemustine in patients with melanoma. *Eur. J. Cancer*, **29**, 711–719.
14. Eisenbrand, G. and Habs, M. (1980) Chronic toxicity of cytostatic N-nitroso-(2-chloroethyl)-ureas after repeated intravenous application in rats. In Holmstedt et al. (eds), *Mechanisms of toxicity and hazard evaluation*. pp. 273–278.
15. Boutin, J.A., Norbreck, K., Moldeus, P., Genton, A., Paraire, M., Bizzari, J.P., Lavielle, G. and Cudenne, C.A. (1989) Effects of the new nitrosourea derivative fotemustine on the glutathione reductase activity in rat tissues *in vivo* and in isolated rat hepatocytes. *Eur. J. Cancer Clin. Oncol.*, **25**, 1311–1316.
16. Schallreuter, K.U., Gleason, F.K. and Wood, J.M. (1990) The mechanism of action of the nitrosourea anti-tumor drugs on thioredoxin reductase, glutathione reductase and ribonucleotide reductase. *Biochim. Biophys. Acta*, **1054**, 14–20.
17. Brakenhoff, J.P.G., Commandeur, J.N.M., de Kanter, F.J.J., van Baar, B.L.M., Luijten, W.C.M.M. and Vermeulen, N.P.E. (1994) Chemical and glutathione conjugation-related degradation of fotemustine: formation and characterization of a glutathione conjugate of diethyl(1-isocyanatoethyl) phosphonate a reactive metabolite of fotemustine. *Chem. Res. Toxicol.*, **7**, 380–389.
18. Brakenhoff, J.P.G., Commandeur, J.N.M., Lamorée, M.H., Dubelaar, A.C., van Baar, B.L.M., Lucas, C. and Vermeulen, N.P.E. (1993) Identification and quantitative determination of glutathione-related urinary metabolites of fotemustine, a new anti-cancer agent. *Xenobiotica*, **23**, 935–947.
19. Slatter, J.G., Davis, M.R., Han, D.-H., Pearson, P.G. and Baillie, T.A. (1993) Studies on the metabolic fate of carbamide, an experimental antitumor agent in the rat. Evidence for the release of methyl isocyanate *in vivo*. *Chem. Res. Toxicol.*, **6**, 335–340.
20. Stahl, W., Lenhardt, S., Przybylski, M. and Eisenbrand, G. (1992) Mechanism of glutathione-mediated DNA damage by the antineoplastic agent 1,3-bis(2-chloroethyl)-N-nitrosourea. *Chem. Res. Toxicol.*, **5**, 106–109.
21. Stahl, W. (1987) Untersuchungen zur reaktion von 2-chloroethylnitrosourea-harnstoffen doctoral thesis, department of food chemistry and environmental toxicology, Kaiserslautern, Germany.
22. Jefcoate, C.R. (1978) Measurement of substrate and inhibitor binding to microsomal cytochrome P450. *Method Enzymol.*, **52**, 258–279.
23. Sazuka, Y., Tanizawa, H. and Takino, Y. (1989) Effect of adriamycin on the activities of superoxide dismutase, glutathione peroxidase and catalase in tissues of mice. *Jpn J. Cancer Res.*, **80**, 89–94.
24. Paglia, D.E. and Valentine, W.N. (1967) Studies on quantitative and qualitative characterization of erythrocyte glutathione peroxidase. *J. Lab. Clin. Med.*, **70**, 158–169.
25. Worthington, D.J. and Rosemeyer, M.A. (1974) Purification of the crystalline enzyme from erythrocytes. *Eur. J. Biochem.*, **48**, 167–177.
26. Habig, W.H., Pabst, M.J. and Jacoby, W.B. (1974) The first enzymatic step in mercapturic acid formation. *J. Biol. Chem.*, **249**, 7130–7139.
27. Haenen, G.R.M.M., Vermeulen, N.P.E., Timmerman, H. and Bast, A. (1989) Effects of thiols on lipid peroxidation in rat liver microsomes. *Chem. - Biol. Interactions*, **71**, 201–212.
28. Nagelkerke, J.F., Barto, K.P. and van Berkel, T.J.C. (1983) *J. Biol. Chem.*, **258**, 12221–12227.
29. van de Straat, R., de Vries, J., Debets, A.J.J. and Vermeulen, N.P.E. (1987) *Biochem. Pharmacol.*, **36**, 2065–2070.
30. Redegeld, F.A.M., van Opstal, M.A.J., Houdkamp, E. and van Bennekom, W.P. (1988) Determination of glutathione in biological material by flow-injection analysis using an enzyme recycling reaction. *Analyt. Biochem.*, **174**, 489–495.
31. Bruggeman, I.M., Temmink, J.H.M. and van Bladeren, P.J. (1986) Glutathione- and cysteine-mediated cytotoxicity of allyl and benzyl isothiocyanate. *Toxicol. Appl. Pharmacol.*, **83**, 349–359.
32. Slatter, J.G., Rashed, M.S., Pearson, P.G., Han, D.-H. and Baillie, T.A. (1991) Biotransformation of methyl isocyanate in the rat. Evidence for glutathione conjugation as a major pathway of metabolism and implications for isocyanate-mediated toxicities. *Chem. Res. Toxicol.*, **4**, 157–161.
33. Cerami, A. and Manning, J.M. (1971) Potassium cyanate as an inhibitor of the sickling of erythrocytes *in vitro*. *Proc. Natl Acad. Sci. USA*, **68**, 1180–1183.
34. Comporti, M. (1989) Three models of free radical-induced cell injury. *Chem. - Biol. Interactions*, **72**, 1–56.
35. Comporti, M. (1987) Glutathione depleting agents and lipid peroxidation. *Chem. Phys. Lipids*, **45**, 143–169.
36. Bast, A. and Haenen, G.R.M.M. (1984) Cytochrome P-450 and glutathione, what is the significance of their interrelationship in lipid peroxidation. *Trends Biochem. Sci.*, **9**, 510–513.
37. Jones, D., Thor, H., Smith, M.T., Jewell, S.A. and Orrenius, S. (1983) Inhibition of ATP-dependent microsomal Ca^{2+} sequestration during oxidative stress and its reversion against glutathione. *J. Biol. Chem.*, **258**, 6390–6393.
38. Di Monte, D., Bellomo, G., Thor, H., Nicotera, P. and Orrenius, S. (1984) Medianone-induced cytotoxicity is associated with protein thiol oxidation and alteration in intracellular Ca^{2+} homeostasis. *Arch. Biochem. Biophys.*, **235**, 343–350.
39. Bellomo, G., Mirabelli, F., Richelmi, P. and Orrenius, S. (1983) Critical role of sulfhydryl groups in the ATP-dependent Ca^{2+} sequestration by the plasma membrane fraction from the rat liver. *FEBS Lett.*, **163**, 136–139.
40. Thor, H., Hartzell, P., Svensson, S.A., Orrenius, S., Mirabelli, F., Marinoni, V. and Bellomo, G. (1985) The role of thiol groups in the inhibition of liver microsomal Ca^{2+} sequestration by toxic agents. *Biochem. Pharmacol.*, **34**, 3717–3723.
41. Bast, A., Leurs, R. and Timmerman, H. (1989) Cyclandelate as a calcium modulating agent in rat cerebral cortex. *Drugs*, **33**, 67–74.
42. Prohaska, J.R. (1980) The glutathione peroxidase activity of the glutathione-S-transferases. *Biochim. Biophys. Acta*, **611**, 157–174.
43. Khayat, D., Lokiec, F., Bizzari, J.P., Weil, M., Meeus, L., Sellami, M., Rousseau, J., Banzet, P. and Jacquillat, C. (1987) Phase I clinical study of the amino acid-linked nitrosourea, S 10036, administered on a weekly schedule. *Cancer Res.*, **47**, 6782–6785.
44. Commandeur, J.N.M., Stijntjes, G.J. and Vermeulen, N.P.E. (1995) Enzymes and transport systems involved in the formation and disposition of glutathione-S-conjugates. *Pharmacol. Rev.*, **47**, 271–336.
45. Jochheim, C.M. and Baillie, T.A. (1994) Selective and irreversible inhibition of glutathione reductase *in vitro* by carbamate thioester conjugates of methyl isocyanate. *Biochem. Pharmacol.*, **48**, 1197.
46. Kassahun, A. et al. (1994) Effects of carbamate thioester derivatives of methyl and 2-chloroethyl isocyanate on glutathione levels and glutathione reductase activities in the rat. *Biochem. Pharmacol.*, **48**, 587.
47. Shinohara, K. and Tanaka, K.R. (1979) Mechanism of inhibition of red blood cell glutathione reductase activity by BCNU (1,3-bis(2-chloroethyl)-1-nitrosourea). *Clin. Chim. Acta*, **92**, 147–152.
48. Stahl, W. and Eisenbrand, G. (1991) Comparative study on the influence of two 2-chloroethylnitrosoureas with different carbamoylating potential towards glutathione and glutathione related enzymes in different organs in the rat. *Free Rad. Res. Commun.*, **14**, 271–278.
49. Kann, H.E. (1981) Carbamoylating activity of nitrosoureas. In Prestakyo, A.W. et al. (eds), *Nitrosoureas: current status and new developments*. Academic Press, New York, pp. 95–105.
50. Ali-Osman, F., Ginlin, J., Berger, M., Murphy, M. and Rosenblum, M. (1985) Chemical structure of carbamoylating groups and their relationships to

- bone marrow toxicity and antiglioma activity of bifunctional alkylating and carbamoylating agents. *Cancer Res.*, **45**, 4185–4191.
51. Karplus, P.A., Krauth-Siegel, R.L., Schirmer, R.H. and Schultz, G.E. (1988) Inhibition of human glutathione reductase by the nitrosourea drugs 1,3-bis(2-chloroethyl)-1-nitrosourea and 1-(2-chloroethyl)-3-(2-hydroxyethyl)-1-nitrosourea. *Eur. J. Biochem.*, **171**, 193–198.
52. Tew, K.D., Dean, S.W. and Gibson, N.W. (1987) The effect of a novel taurine nitrosourea, 1-(2-chloroethyl)-3-[2-(dimethylaminosulfonyl)ethyl]-1-nitrosourea (TCNU) on cytotoxicity, DNA crosslinking and glutathione reductase in lung carcinoma cell lines. *Cancer Chem. Pharmacol.*, **19**, 291–295.
53. Jeevaratnam, K., Vidya, S. and Vaidyanathan, C.S. (1993) Role of lipid peroxidation in impairment of mitochondrial function at complex I by methylisocyanate treatment of rats *in vivo*. *Biochem. Mol. Biol. Int.*, **30**, 411–417.
54. Meredith, M.J. and Reed, D.J. (1983) Depletion *in vitro* of mitochondrial glutathione in rat hepatocytes and enhancement of lipid peroxidation by adriamycin and 1,3-bis(2-chloroethyl)-1-nitrosourea (BCNU). *Biochem. Pharmacol.*, **32**, 1383–1388.
55. Vermeulen, N.P.E., den Kelder, D.-O. and Commandeur, J.N.M. (1993) Formation and protection against toxic reactive intermediates. In Tesla, B., Kyburz, E., Fuhrer, W. and Giger, R. (eds), *Perspectives in medicinal chemistry*. Verlag Helvetica Chimica Acta, Basel, Switzerland, pp. 573–593.

Received on October 30, 1995; revised on January 8, 1996; accepted on January 10, 1996